ESA Cloud_cci

Algorithm Theoretical Baseline Document

Issue 9 Revision 0

20.11.2023

Deliverable No.:	D-2.1
ESRIN/Contract No.:	4000128637/20/I-NB
Project Coordinator:	Dr. Martin Stengel Deutscher Wetterdienst martin.stengel@dwd.de
Technical Officer:	Michael Eisinger European Space Agency Michael.Eisinger@esa.int
DOIs of Cloud_cci datasets:	N/A

Document Change Record

Document, Version	Date	Changes	Originator
ATBD Version 6.0	30/10/2018	Revision wrt. this document representing algorithms (CC4CL) and Level 3 tools used for processing of AVHRR-AM/PMv3 and ATSR2-AATSRv3 datasets • Updating Section 1, in particular sub section 1.2 and 1.3 to represent data set versions 3. • Removing outdated information from Section 2 • Updated Section 3: - updated information on cloud detection and cloud phase - adding subsection 3.4 on the calculation of broadband fluxes • Adding Section 4.2.3 on the aggregation of broadband flux properties.	M. Stengel
ATBD Version 6.1	05/02/2019	Updates after ESA review of document version 6.0. E.g.: • Revising subsection 3.1 • Minor edits to subsections 3.2 and 3.3 • Minor updates to section 4	M. Stengel
ATBD Version 6.2	12/03/2019	Updates after ESA review of document version 6.1.E.g. • Adding a comment on BB flux uncertainties • Adding Section 1.4 (copy/paste from PVIRv5) for consistency between ATBD, PUG, and PVIR	M. Stengel
ATBD Version 7.0	22/03/2021	First version of Cloud_cci+ Phase1 including • Revising the introduction to account for the current project phase • Adding information on SEVIRI and SLSTR • Removed information on AVHRR and AATSR in this version	M. Stengel & PT
ATBD Version 7.1	29/09/2021	Adding technical description of output data+format (new Section 5 + new Annex A)	M. Stengel
ATBD Version 8.0 submitted	12/09/2022	• Changing ESA Technical Officer • Minor editing to account for new document versions	M. Stengel
ATBD Version 8.1	24/11/2022	• Revising section 3.5	M. Stengel
ATBD Version 9.0	20/11/2023	Final and approved version	M. Stengel

Purpose

The purpose of the Cloud_cci Algorithm Theoretical Baseline Documents (ATBDs) is to document the theoretical background of all components of the algorithms used for the generation of the Cloud_cci's SEVIRI and SLSTR data. This document focusses on overarching aspects with in-depth information on the retrieval itself being given in ATBD-CC4CLv9.0.

Table of Contents

1. Introduction

1.1 The ESA Cloud_cci project – previous phases

The ESA Cloud_cci project covers the cloud component in the European Space Agency's (ESA) Climate Change Initiative (CCI) programme (Hollmann et al., 2013). In the ESA Cloud_cci project, long-term and coherent cloud property datasets have been generated exploiting the synergic capabilities of different Earth observation missions (European and non-European) allowing for improved accuracies and enhanced temporal and spatial sampling better than those provided by the single sources. The Cloud_cci datasets are the attempt to respond to GCOS requirements for the Cloud Properties Essential Climate Variable (ECV).

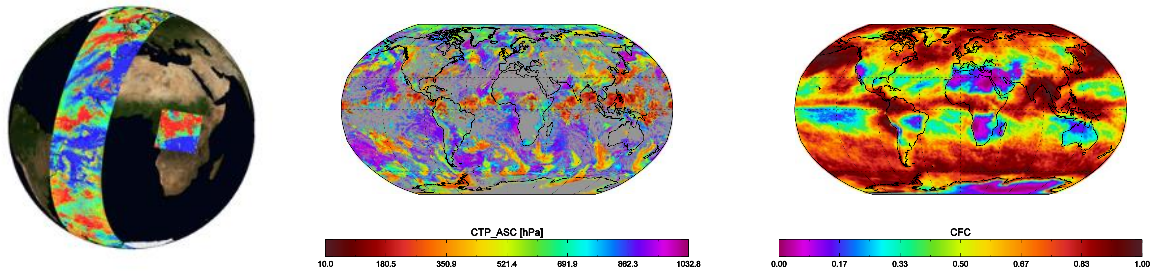

Figure 1-1 *Examples of Cloud_cci cloud products. Left: Pixel-based (Level 2), middle: daily composite on a global grid (Level 3U), right: monthly averaged on a global grid (Level 3C)*

To make the Cloud_cci datasets improved compared to existing ones, the following two essential steps were undertaken in previous project phase (CCI Cloud Phase I & II):

1) Revisit the measurement data (Level-1) and corresponding calibration performance and development of a carefully inter-calibrated and rigorously quality checked radiance data sets for AVHRR, so called Fundamental Climate Data Record (FCDR). Within this effort the calibration of AVHRR, MODIS and AATSR was compared and characterized. Please see the ATBDv5 for more information about all sensors used and their imaging characteristics. More information on the AVHRR FCDR produced and used is available in RAFCDRv1.0.

2) Development of two state-of-the-art physical retrieval systems that use the optimal estimation technique for a simultaneous, spectrally consistent retrieval of cloud properties including pixel-based uncertainty measures. The first retrieval framework is the Community Cloud retrieval for Climate (CC4CL; Sus et al., 2017; McGarragh et al., 2017) which is applied to AVHRR and AVHRR-heritage channels (i.e. channels which are available from all sensors) of MODIS and AATSR. The second retrieval framework is the Freie Universität Berlin AATSR MERIS Cloud retrieval (FAME-C; Carbajal Henken et al., 2014) and is applied to synergistic MERIS and AATSR measurements on-board of ENVISAT.

Based on these developments, multiple multi-annual, global datasets of cloud properties were generated using the passive imager satellite sensors AVHRR, MODIS, (A)ATSR and MERIS. These datasets were comprehensively evaluated (1) by using accurate reference observations of ground stations and space-based Lidar measurements and (2) by comparisons to existing and well-established global cloud property datasets.

These datasets were published as **version 2** and version 3 and associated Digital Object Identifiers were issued:

DOI:10.5676/DWD/ESA_Cloud_cci/AVHRR-PM/V002
DOI:10.5676/DWD/ESA_Cloud_cci/AVHRR-AM/V002
DOI:10.5676/DWD/ESA_Cloud_cci/MODIS-Terra/V002
DOI:10.5676/DWD/ESA_Cloud_cci/MODIS-Aqua/V002
DOI:10.5676/DWD/ESA_Cloud_cci/ATSR2-AATSR/V002
DOI:10.5676/DWD/ESA_Cloud_cci/MERIS+AATSR/V002

DOI:10.5676/DWD/ESA_Cloud_cci/AVHRR-PM/V003
DOI:10.5676/DWD/ESA_Cloud_cci/AVHRR-AM/V003
DOI:10.5676/DWD/ESA_Cloud_cci/ATSR2-AATSR/V003

A comprehensive set of corresponding documentation is available through https://climate.esa.int/en/projects/cloud/key-documents/

1.2 Cloud_cci+ Phase I

ESA Cloud_cci+ was kicked off in March 2020. Cloud_cci contribute to and improves on the successful efforts of Cloud_cci: the development, validation and application of novel cloud property data sets maximising the use of ESA and other European EO mission data and targeting the GCOS requirements for the Cloud ECV. The ultimate goal of the ESA Cloud_cci+ is the improvement of retrieval algorithms and processing concepts and implementations, and the development of two novel data sets based on measurements form the Spinning Enhances Visible and Infrared Imager (SEVIRI) and from Sea and Land Surface Temperature Radiometer (SLSTR). The processing systems will have the potential to be used for ensuring a sustainable provision of such data from operational entities through for instance the EUMETSAT SAF network and the Copernicus Climate Change Service after the initial R&D under the ESA CCI programme has been completed.

Focus of the further CC4CL development will be on:

- Enhance the CC4CL capabilities wrt. utilizing the advanced spectral information available from SEVIRI and SLSTR compared to AVHRR-heritage.
- Improvement of Cloud detection over snow and ice surfaces (e.g. in polar regions), in mountainous regions and in the presence of optically thin cirrus clouds
- Improvement of cloud phase determination and the detection of multi-layer cloud situations as knowledge of both aspects significantly impacts the subsequent retrieval of cloud properties
- Improvement of the uncertainty

A full list of planned developments is given (and regularly updated) in the Algorithm Development Plan (ADPv3.0)

The cloud products retrieved from SEVIRI and SLSTR remain the same compared to previous datasets and are outlined in the next subsection.

1.3 Cloud_cci cloud products

The cloud properties derived on pixel level of each utilized sensor are listed in Table 1-1. It is important to note that the cloud properties CLA, LWP, IWP are not directly retrieved, but rather determined from retrieved COT and CER in a post processing step. The same applies to CTH and CTT, which are inferred from the retrieved CTP. In addition, it needs to be noted that for the determination of radiative fluxes a fair amount of ERA5 data is required.

Based on the pixel level retrievals the data is further processed into different processing levels as summarized in Table 1-2. Level-3U denotes a global composite on a global Latitude-Longitude grid (of 0.05° resolution) onto which the Level-2 data is sampled (see Section 4.1 for more details on Level-3U sampling). Level-3C products are also defined on Latitude-Longitude grid (here 0.5° resolution) onto which the properties are averaged or their frequency collected (histograms). Further separation of cloud properties in Level-3C in e.g. day/night, liquid/ice, were made wherever suitable (see* Level-3U data are only provided for SLSTR

Table 1-3).

Table 1-1 *List of generated cloud properties. CMA/CFC and CPH are derived in a pre-processing step. In the next step, COT, CER and CTP are retrieved simultaneously by fitting a physically consistent cloud/atmosphere/surface model to the satellite observations using optimal estimation (OE). Moreover, LWP and IWP are obtained from COT and CER. In addition, spectral cloud albedo (CLA) for two visible channels are derived. In a post-processing step, derived cloud properties and ERA-Interim information are used to determine radiative broadband fluxes. The Photosynthetically active radiation (PAR) is no standard output.*

Variable	Abbrev.	Definition
Cloud mask / Cloud fraction	CMA/ CFC	A binary cloud mask per pixel (L2, L3U) and therefrom derived monthly total cloud fractional coverage (L3C) and separation into 3 vertical classes (high, mid-level, low clouds) following ISCCP classification (Rossow and Schiffer, 1999).
Cloud phase	CPH	The thermodynamic phase of the retrieved cloud (binary: liquid or ice; in L2, L3U) and the therefrom derived monthly liquid cloud fraction (L3C).
Cloud optical thickness	COT	The line integral of the absorption coefficient and the scattering coefficient (at 0.55µm wavelength) along the vertical in cloudy pixels.
Cloud effective radius	CER	The area-weighted radius of the cloud drop and crystal particles, respectively.
Cloud top pressure/ height/ temperature	CTP/ CTH/ CTT	The air pressure [hPa] /height [m] /temperature [K] of the uppermost cloud layer that could be identified by the retrieval system.
Cloud liquid water path/ Ice water path	LWP/ IWP	The vertical integrated liquid/ice water content of existing cloud layers; derived from CER and COT. LWP and IWP together represent the cloud water path (CWP)
Joint cloud property histogram	JCH	This product is a spatially resolved two-dimensional histogram of combinations of COT and CTP for each spatial grid box.
Spectral cloud albedo	CLA	The blacksky cloud albedo derived for channel 1 (0.67 µm) and 2 (0.87 µm), respectively (experimental product)
Cloud effective emissivity	CEE	cloud radiative thickness in the infrared typically referred

Variable	Abbrev.	Definition
		to as the "effective emissivity"
Top of atmosphere upwards/downwards flux	TOA	Shortwave (SW) and longwave (LW) fluxes at the Top of the atmosphere, upwelling and downwelling
Top of atmosphere upwards/downwards flux - clear-sky	TOA_{clear}	Shortwave (SW) and longwave (LW) fluxes at the Top of the atmosphere, upwelling and downwelling - for clear sky conditions
Bottom of atmosphere (surface) upwards/downwards flux	BOA	Shortwave (SW) and longwave (LW) fluxes at the Bottom of the atmosphere, upwelling and downwelling
Bottom of atmosphere (surface) upwards/downwards flux - clear-sky	BOA_{clear}	Shortwave (SW) and longwave (LW) fluxes at the Bottom of the atmosphere, upwelling and downwelling - for clear sky conditions
Photosynthetically active radiation	PAR	Bottom of atmosphere incoming shortwave radiation in the spectral range between 400 and 700nm

Table 1-2 *Processing levels of Cloud_cci data products. Level-3U and Level-3Care each directly derived from Level-2.*

Processing level	Spatial resolution	Description
Level-2 (L2)	SLSTR: 1km SEVIRI: 3-5 km	Retrieved cloud variables at satellite sensor pixel level, thus with the same resolution and location as the sensor measurements (Level-1)
Level-3U* (L3U)	Latitude-Longitude grid at 0.05° res.	Cloud properties of Level-2 orbits projected onto a global space grid without combining any observations of overlapping orbits. Only subsampling is done. Common notation for this processing level is also L2b. Temporal coverage is 24 hours (0-23:59 UTC).
Level-3C (L3C)	Latitude-Longitude grid at 0.5° res.	Cloud properties of Level-2 orbits of one single sensor combined (averaged / sampled for histograms) on a global space grid. Temporal coverage of this product is 1 month.

* Level-3U data are only provided for SLSTR

Table 1-3 *Cloud_cci product features incl. day and night separation, liquid water and ice as well as histogram representation. Level-3U refers to the un-averaged, pixel-based cloud retrievals sampled onto a global Latitude-Longitude (lat/lon) grid. [1]CMA in Level-2 and Level-3U is a binary cloud mask. All products listed exist in each dataset listed above.*

	Level 2 **swath based** 1km/5km	**Level-3U** **daily sampled** **global** 0.05° lat/lon grid	**Level-3C** **monthly averages** **global** 0.5° lat/lon grid	**Level-3C** **monthly histograms** **global** 0.5° lat/lon grid
CMA/CFC	✓ as CMA[1]	✓ as CMA[1]	✓day/night/high/mid/low	-

CTP, CTH, CTT	✓	✓	✓	✓ liquid/ice
CPH	✓	✓	✓ day/night	-
COT	✓	✓	✓ liquid/ice	✓ liquid/ice
CER	✓	✓	✓ liquid/ice	✓ liquid/ice
LWP	✓ as CWP	✓ as CWP	✓	✓ as CWP
IWP			✓	
CLA	✓ 0.6/0.8µm	✓ 0.6/0.8µm	✓ 0.6/0.8µm	✓ 0.6/0.8µm/liquid/ice
JCH	-	-	-	✓ liquid/ice
$TOA_{up,dn,sw,lw}$	✓	✓	✓	-
$BOA_{up,dn,sw,lw}$, PAR	✓	✓	✓	-

2. Satellite sensors used

The two passive imaging sensors SEVIRI and SLSTR are the focal point in the current CCI+ Clouds Phase I. Both sensors and corresponding data briefly introduced in the following.

2.1 SEVIRI

Sensor characteristics

SEVIRI is a passive optical imaging radiometer with 12 spectral channels at visible and infrared wavebands (see Table 2-2). SEVIRI instruments are mounted on the geostationary MSG satellites and measure from 2004 onwards. MSG 1, MSG 2, MSG 3 and MSG 4 measurement images are to align to each other and centred at 0°/0° longitude/latitude. The region seen by a SEVIRI covers Africa, Europe, partly South America, the Atlantic Ocean and the Middle East. All four SEVIRI instruments on MSG 1, MSG 2, MSG 3 and MSG 4 are identical in construction. The SEVIRI imaging repeat cycle is 15 minutes.

SEVIRI data record used in Cloud_cci

SEVIRI Level 1b is procured from EUMETSAT through CM SAF. Before being used in CC4CL, SEVIRI L1B infrared channels were calibrated using the Global Space-based Inter-Calibration System (GSICS) calibration. Visible channels are calibrated using the NASA coefficients (Doelling, 2018).

2.1 SLSTR

Sensor characteristics

The SLSTR (Sea and Land Surface Temperature Radiometer) sensor is a 11-channel passive imaging sensor with dual viewing directions for accurate atmospheric corrections. SLSRT channels are spectrally located between 0.55 and 12.00 µm. Focus of SLSTR is multi-purpose VIS/IR imagery, with emphasis for example on surface temperature and cloud property retrievals. Precursor sensors are ATSR. ATSR2 and AATSR on board ERA, ERS-2 and Envisat. SLSTR is a payload of the Sentinel-3 satellite which was launched in February 2016. SLSTR swath with is 1400 km for cross-nadir and 740 km for aft-viewing swath. Spatial footprint size of one pixel is 0.5 km for short-wave channels and 1.0 km for IR channels. Table 2-1 lists the SLSTR channels.

Table 2-1 *SLSTR spectral channels*

Channel	Wavelength [nm]	Bandwidth [nm]
1	550	20
2*	665	20
3*	865	20
4	1375	
5	1610	60
6	2250	
7*	3740	380
8*	10850	900
9*	12000	1000

* AVHRR-heritage channels of SLSTR used in CC4CL

SLSTR data record used in Cloud_cci

Level 1b data of SLSTR is used in Cloud_cci. Data identifier: SL1_RBT at Near Real Time (NRT).

Table 2-2 *SEVIRI channel characteristics (source: EUMETSAT, 2010)*

Channel ID	**Absorption Band / Channel Type**	**Nominal Centre Wavelength (µm)**	**Spectral Bandwidth (µm)**	**Dynamic Range**	**Spectral Bandwidth** As % of energy actually detected within spectral band
HRV	Visible High Spatial Resolution	Nominally 0.75	0.6 to 0.9	0 - 459 W/(m2 sr µm) (scaled at centre frequency)	Precise spectral characteristics not critical
VIS 0.6	VNIR Core Imager	0.635	0.56 to 0.71	0 - 533 W/(m2 sr µm)	98.0 %
VIS 0.8	VNIR Core Imager	0.81	0.74 to 0.88	0 - 357 W/(m2 sr µm)	99.0 %
IR 1.6	VNIR Core Imager	1.64	1.50 to 1.78	0 - 75 W/(m2 sr µm)	99.0 %
IR 3.9	IR / Window Core Imager	3.92	3.48 to 4.36	0 - 335 K	98.6 %
IR 6.2	Water Vapour Pseudo-Sounding	6.25	5.35 to 7.15	0 - 300 K	99.0 %
IR 7.3	Water Vapour Pseudo-Sounding	7.35	6.85 to 7.85	0 - 300 K	98.0 %
IR 8.7	IR / Window Core Imager	8.70	8.30 to 9.10	0 - 300 K	98.0 %
IR 9.7	IR / Ozone Pseudo-Sounding	9.66	9.38 to 9.94	0 - 310 K	99.0 %
IR 10.8	IR / Window Core Imager	10.80	9.80 to 11.80	0 - 335 K	98.0 %
IR 12.0	IR / Window Core Imager	12.00	11.00 to 13.00	0 - 335 K	98.0 %
IR 13.4	IR / Carbon Dioxide Pseudo-Sounding	13.40	12.40 to 14.40	0 - 300 K	96.0 %

3. The Community Cloud retrieval for CLimate (CC4CL) retrieval system

CC4CL consists of three main components: cloud detection, cloud typing and OE-based cloud property retrieval, which are summarized in the following subsections. As a post-processing step, radiative broadband flux properties are derived.

3.1 Cloud detection

The cloud detection is based on artificial neural networks (ANNs) that have been trained using AVHRR-heritage channel (applied SLSTR) and using SEVIRI (applied to SEVIRI) measurements and collocated CALIOP cloud optical depth (COD) for a subset of all available CALIOP-AVHRR-NOAA18/19 collocation in 2007 to 2014. The applied ANN outputs mimicked CALIOP COD (ANNCOD) in the range of 0 to 1. To convert the ANNCOD to a needed binary cloud decision, thresholds are applied which depend on illumination conditions (day/night/twilight) and region (land/sea). Verification scores were calculated, using the training data set, based on the ANNCOD output and the threshold applied, which are used to determine the uncertainty of the cloud mask decision per pixel.

More information about the cloud detection can be found in ATBD-CC4CLv9.0.

3.2 Cloud typing & phase

Typing

Cloud typing is based on developments by Pavolonis and Heidinger (2004) and Pavolonis et al. (2005), which is based on a threshold decision tree. Cloud type output classes are:

- clear
- switched to water* (liquid)
- fog (liquid)
- water (liquid)
- supercooled (liquid)
- switched to ice* (ice)
- opaque ice (ice)
- cirrus (ice)
- deep convective (ice)
- overlap (ice)

The classes switched-to-water and switched-to-ice are additional classes introduced by Cloud_cci which account for too warm ice clouds (according to CTT) being reclassified to water and too cold liquid clouds being reclassified as ice.

Phase

An artificial neural network was trained and is applied to SEVIRI and SLSTR for the phase determination. Similar to the cloud detection, one ANN for cloud phase received input by collocating AVHRR measurements (this is applied to the AVHRR-heritage channels of SLSTR), the other using SEVIRI measurement. Both neural networks are trained against CALIOP cloud-top phase information. The output of the ANNs range from 0 to 1, imposing the need for applying a threshold to the output to infer a binary phase information. Exact input setting and the thresholds reported in ATBD-CC4CLv9.0.

3.3 Optimal estimation retrieval of cloud properties

The CC4CL retrieval of cloud properties is based on ORAC (Optimal Retrieval of Aerosol and Cloud) algorithm (Poulsen et al., 2012 and Watts et al., 1998, but including further developments made in the Cloud_cci Project: Sus et al. (2017), McGarragh (2017) and ATBD-CC4CLv9.0). The retrieval is based on the optimal estimation technique and can be used to determine both aerosol and cloud properties from visible/infrared satellite radiometers. In the case of cloud retrievals the algorithm, models the surface properties, atmosphere and subsequent fits the cloud properties using LUTs created from DIScrete Ordinates Radiative Transfer (DISORT) (Stamnes et al. 1998) to the TOA signal measured by the satellite by varying the cloud optical depth, effective radius, cloud top pressure, phase and surface temperature. From these retrieved products we can subsequently derive liquid and ice water path. The optimal estimation framework of CC4CL provides some key advantages such as

- Comprehensive propagation of the measurement and forward model error into the final product.
- The ability to include prior knowledge of the retrieved quantities together with the uncertainties in a priori knowledge.
- A mathematically rigorous estimate of the uncertainty on retrieved values on a pixel by pixel basis by propagating the uncertainties of the measurements, model and a priori data.
- The retrieval also provides an indicator (‘the cost’) of the appropriateness of the model used.

A specific advantage of this algorithm is that it uses all channels and derives all parameters simultaneously. Hence the algorithm provides a measure of the consistency between retrieval representation of cloud and satellite radiance. The current version of CC4CL uses ORAC with RTTOV to calculate the clear sky radiances in the visible and infrared. The derived pixel level cloud properties are listed in Table 1-1, of which CTP, COT, CER are part of the state vector in the optimal estimation, while all others are derived. A summary is given in Table 3-1. More detailed information on the ORAC system can be found in McGarragh (2017) and ATBD-CC4CLv9.0, with the latter also holding information about recent developments,

3.4 Calculation of the broadband fluxes

Broadband radiative fluxes are computed in a post-processing step of the CC4CL using BUGSrad (Stephens et al., 2001). BUGSrad is based on the two-stream approximation and correlated-k distribution methods of atmospheric radiative transfer. The basis of the algorithm is the same as that described by Fu and Liou (1992). It is applied to a single-column atmosphere for which the cloud and aerosol layers are assumed to be plane-parallel. Cloud properties retrieved using CC4CL are ingested into BUGSrad to compute both shortwave and longwave radiative fluxes for the top and bottom of atmosphere. The algorithm uses 18 bands that span the entire electromagnetic spectrum to compute the broadband flux. In total, 6 bands are used for shortwave and 12 bands are used for longwave radiative flux calculations. In depth information about BUGSrad and its application can be found in ATBD-CC4CL-TOA_FLUXv1.1. Comparisons to surface and other satellite data were presented in Stengel et al. (2019) using the AVHRR-PMv3 dataset.

3.5 Limitations

A full list of the assumptions and uncertainties are outlined in the uncertainty characterisation document (CECRv4). The main assumptions are listed below.

1. Although the CC4CL cloud algorithm is capable of utilizing the individual spectral information of each implemented sensor, some modules will only utilize the information of the AVHRR heritage channels. .
2. The CC4CL cloud model assumes a single layer of cloud. Per default, no a-priori climatological information is used in the retrieval to constrain the cloud heights hence the cloud height retrieved is the radiative effective cloud height in the case of multi-layer clouds. However, work is ongoing to implement the utilization of a-priori CTP information as both first guess and/or a-priori in the optimal estimation.

3. The CC4CL cloud retrieval uses the IR channels to assign the cloud height. The penetration depth of the IR clouds is approximately 1 optical depth into the cloud layer. The cloud height assignment and associated phase will be influenced by this, typically leading to an overestimation of the derived cloud top pressure (underestimation of cloud top height). An attempt to account for the semi-transparency of many uppermost cloud layers is documented in Section 2.3.10 of ATBD-CC4CLv9.0.
4. The effective radius and optical depth retrievals are strongly dependent on the choice of optical properties used. The effective radius will also differ depending on whether 1.6 and 3.7µm channel information is used if the vertical profile of effective radius changes with height. The 1.6µm channel penetrates deeper into the cloud.

Table 3-1 *CC4CL in a nutshell.*

	CC4CL
History	ORAC which was originally developed for application to SEVIRI (OCA, P. Watts). Applied to ATSR under nationally funded project GRAPE by RAL and University of Oxford. Further developed in ESA Cloud_cci to be applicable to AVHRR, MODIS, AATSR, SEVIRI and successor sensors.
COT CER CTP	1. All cloud parameters retrieved simultaneously. NWP profiles calculated using RTTOV 2. Post correction of CTP/CTH for boundary layer inversion situations 3. Vis/NIR LUTS derived using DISORT RTM
LWP	LWP=4/3 (τ*re*ρwat/Qwat) ; Qwat=2 (τ: optical thickness, re: effective radius, ρwat: density liquid water)
IWP	IWP=4/3 (τ*re*ρice/Qice) ; Qice=2.1 (τ: optical thickness, re: effective radius, ρice: density ice water)
Ice	Baum Ice crystals
Phase Discrimination	Cloud typing is based on Pavolonis et al. (2005), cloud phase is based on ANN with posterior application of scene dependent thresholds to derived a binary phase information.
Cloud Mask	An ANN based retrieval is applied to all pixels including a posterior application of scene dependent threshold to the ANN output of a pseudo CALIPSO COD yielding into a binary cloud mask information.
Broadband fluxes	Using the retrieved properties CER, COT, CTP and Stemp in addition to thermodynamic profiles from reanalysis data, broadband fluxes are calculated at TOA and BOA (upwelling+downwelling, shortwave+longwave) at each satellite pixel.
Snow/Ice discrimination	Snow and sea ice information is used from the NSIDC data base. Alternatively, ERA-Interim snow and ice information can be chosen. The information is used to modify the surface albedo.
Errors Quality Control	Cost function provides an indication of the quality of the fit to the cloud model. If the fit is good then the errors indicate the accuracy of the retrieval. Convergence test: ORAC uses the change in the cost function between iterations to determine whether a retrieval is said to have converged. Errors considered 1. Measurement errors 2. Cloud inhomogeneity 3. Coregistraion error 4. Surface contribution
Comments	Single layer plane parallel cloud assumed for all instruments. State vector also contains surface temperature.

4. Generation of the Level-3 products

The Cloud_cci data products are available at different processing levels including sensor-specific pixel level products (Level-2), sensor-specific global composites (Level-3U) and sensor specific averaged products on a global grid (Level-3C). Details on the processing levels are reported in Table 1-2. All available Level-2 data are input to the Level-3 processing software.

The Level-3U/-3C grid is an equal angle grid covering the full globe. For the L3U sampled product the horizontal resolution is 0.05 degrees, while for Level-3Cthe spatial resolution is 0.5 degrees. The actual gridding is a straightforward process in which the latitude and longitude information of each L2 pixel is used to determine the indices of the corresponding grid cell the pixel falls into. This depends on the desired grid resolution.

The subsections below outline the averaging techniques applied for generation of the Level-3C data.

4.1 Level-3U products

In order to reduce the amount of data and to map the data to a regular grid but without loosing all the horizontal variability by averaging it, a sampling technique has been implemented which is based on choosing the minimum satellite viewing zenith angle. This means that in the final product the pixel with the smallest satellite viewing zenith angle of all pixels falling into the grid cell is chosen to represent that grid cell. This is motivated by the fact that such a pixel is located closest to satellite nadir, which means that undesired effects due to a slant viewing path across the atmosphere are minimal. Since the footprint size increases with increasing satellite viewing angle, the grid cell that are covered by the footprint are calculated individually for each satellite pixel. This leads to that more than one grid cell can be filled with one individual observation depending on footprint size. Additionally, the L3U product is split up in ascending and descending satellite nodes. The viewing zenith angle sampling and the separation into the two nodes effectively leads to a larger temporal and spatial coherence of atmospheric patterns.

4.2 Level-3C products

4.2.1 Aggregating cloud mask and phase information

Cloud mask information consists of three stages: no information available (Fill value), clear (0) and cloudy (1). Averages are produced by counting the instances of clear and cloudy cloud mask information for each grid cell and evaluation of:

$$CC(i,j) = \frac{N(i,j)_{Cloudy}}{N(i,j)_{Cloudy} + N(i,j)_{Clear}}$$

4.2.2 Aggregating microphysical and macrophysical cloud properties

To ensure consistency when averaging the cloud properties, only those pixels are considered for which all cloud variables are available. However, not for all cloudy pixels the cloud retrieval yields valid results, thus the pixels used for averaging cloud properties is usually a subset of those being identified as cloud (and used in the cloud fraction estimation). During night-time apparently no consistence between micro and microphysical properties can be achieved due to the absence of microphysical retrievals.

The unweighted mean and standard deviation for grid cell (i,j) are then defined as:

$$< x(i,j) >= \frac{1}{N(i,j)_{Cloudy}} \sum_{k=1}^{N(i,j)_{Cloudy}} x_k(i,j)$$

$$s(x(i,j)) = (< x^2(i,j) > - < x(i,j) >^2)^{0.5}$$

Where i and j are the longitude and latitude indices. The error weighted mean and standard deviation for grid cell (i,j) are defined as:

$$< x(i,j) >_w = \frac{1}{W_1} \sum_{k=1}^{N(i,j)_{Cloudy}} x_k(i,j) w_k(i,j)$$

$$s(x(i,j))_w = (\frac{W_1}{W_1^2 - W_2} < x^2(i,j) >_w - < x(i,j) >_w{}^2)^{0.5}$$

With:

$$W_1 = \sum_{k=1}^{N(i,j)_{Cloudy}} w_k ; W_2 = \sum_{k=1}^{N(i,j)_{Cloudy}} w_k^2 ; w_k = \frac{1}{\sigma_k}$$

σ_k is the retrieval error of the corresponding variable. This approach is pursued for all micro- and macrophysical variables except for the cloud phase, for which, similar to the cloud cover, the number of liquid cloud instances per grid box is counted and

$$< cty(i,j) >= \frac{N(i,j)_{Cloudy}^{Liquid}}{N(i,j)_{Cloudy}}$$

is computed to give the liquid cloud phase contribution for grid box (i,j). Similar, the liquid and ice water paths are computed as:

$$< lwp(i,j) >= \frac{1}{N(i,j)_{Cloudy}^{Liquid}} \sum_{k=1}^{N(i,j)_{Cloudy}^{Liquid}} cwp_{liquid}$$

$$< iwp(i,j) >= \frac{1}{N(i,j)_{Cloudy}^{Ice}} \sum_{k=1}^{N(i,j)_{Cloudy}^{Ice}} cwp_{Ice}$$

Here, cwp_{Liquid} and cwp_{Ice} are distinguished by the cloud phase flag which is also used in counting the liquid and ice instances for $N(i,j)_{Cloudy}^{Liquid}$ and $N(i,j)_{Cloudy}^{Ice}$. These quantities are therefore connected by:

$$< cwp(i,j) >=< cty(i,j) >< lwp(i,j) > +(1- < cty(i,j) >) < iwp(i,j) >$$

Furthermore, to account for the special structure of the cloud top pressure for this variable the logarithmic average is computed additionally:

$$< ctp(i,j) >_{\ln} = \exp(\frac{1}{N(i,j)_{Cloudy}} \sum_{k=1}^{N(i,j)_{Cloudy}} \ln(ctp_k(i,j)))$$

Apart from those products referring to grid cell averages, 2D ISCCP-like histograms are also produced for each cell which partitions the CTP and COT space.

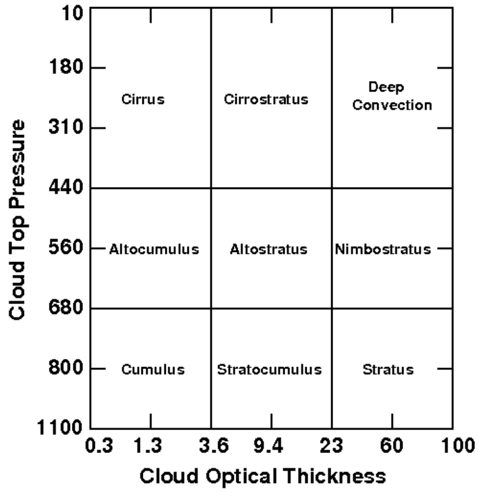

Figure 4-1 *ISCCP-like 2D cloud top pressure vs. cloud optical thickness histogram.*

The widths of the bins are defined as follows:

- COT: {0, 0.3, 0.6, 1.3, 2.2, 3.6, 5.8, 9.4, 15, 23, 41, 60, 80, 100}
- CTP: {1, 90, 180, 245, 310, 375, 440, 500, 560, 620, 680, 740, 800, 875, 950, 1100} [hPa]

As can be seen in Figure 4-1, this partitioning is also associated with nine different cloud types and thus allows for cloud classification of the grid cell.

In addition to the 2D histogram, also 1D histograms are generated for the parameters CTP, CTT, CWP, COT, CER. Each histogram covers the solution space of its variable with the cloud phase as additional dimension. These histograms are provided on the spatial resolution of the level3 averages. The used bins are:

- CWP: {0, 5, 10, 20, 35, 50, 75, 100, 150, 200, 300, 500, 1000, 2000, inf} [g/m^2]
- COT: {0.0, 0.3, 0.6, 1.3, 2.2, 3.6, 5.8, 9.4, 15.0, 23.0, 41.0, 60.0, 80.0, 100}
- CER: {0, 3, 6, 9, 12, 15, 20, 25, 30, 40, 60, 80} [µm]
- CTP:{ 1, 90, 180, 245, 310, 375, 440, 500, 560, 620, 680, 740, 800, 875, 950, 1100} [hPa]
- CTT:{ 200, 210, 220, 230, 235, 240, 245, 250, 255, 260, 265, 270, 280, 290, 300, 310, 350} [K].

4.2.3 Aggregation of broadband fluxes

The aggregation of the broadband fluxes are done in a similar fashion as the aggregation of the cloud properties (see Section 4.2.2), with the exception, that the fluxes are diurnal cycle corrected to represent 24 hour means. This is in particular necessary for shortwave fluxes which heavily depend on the illumination conditions at the time of observation. (The diurnal cycle correction is not applied to SEVIRI data, as the diurnal cycle is already covered by SEVIRI's high temporal resolution.)

Longwave fluxes:

The diurnal cycle of LW fluxes was determined by applying CC4CL to two full days of SEVIRI observations. The mean diurnal cycle, as a function of surface type (land/sea), is then used to determine correction factors, depending on time of the day (thus on the time of observation), which are applied to each individual pixel observation to emulate a 24-hour mean, before averaging.

Shortwave fluxes:

Each shortwave flux observation is related to a specific solar zenith angle impacting the path length though the atmosphere as well as the angle under which the energy is reaching the Earth's surface. Using this information an individual diurnal cycle can be emulated for each pixel by sampling the varying solar zenith angle throughout 24 hours at the pixel location. The rescaled incoming and reflected solar radiation values from all of these samples are averaged to emulate a 24-hour mean for that pixel. This mean is then used to determine monthly means including all observations take at that location throughout the month.

4.2.4 Limitations in the aggregation of Level-3 products

Level 3 generation

As already stated in the text above, all Level-2 data of the month are regarded as equally valid and are summed up to derive the monthly means. Under certain circumstances this could lead to the monthly mean being biased towards days for which more Level-2 data are available compared to others. The applied approach is thus in contrast to weighting each day equally within a month, which on the other hand might lead to few, spatiotemporally isolated observations being weighted too much. Under normal circumstances, under which the data coverage is nearly complete and nearly equally distributed within a month, the results of both approaches do no differ significantly.

Diurnal sampling

The diurnal cycle of clouds is well documented as a source of natural variability in the cloud field. It varies based on cloud type, latitude, season, and location. This cycle has significant effects on the horizontal and vertical distribution of clouds as well as on the cloud microphysical properties. The incomplete sampling of the diurnal cycle by polar orbiting satellite instruments (e.g. SLSTR), where usually 2 observations per day are taken for a specific place on Earth, introduces (1) differences between cloud data records of individual instruments when overpassing at significantly different local time, and (2) generally bias the cloud records compared to climatological means, for which more or less continuous observations within a day a required. By combining the records of the different sensors reduces the sampling error.

For proper interpretation of the temporal variability of individual Cloud_cci data records and among different records it diurnal cycle of cloud cover and possible methods to correct for it were assessed (RODCv1.0). However, Cloud_cci did not attempt to correct the cloud data records for the impact of the diurnal cycle, but rather provide the information. Corrections based on statistical analyses are inherently nonphysical and introduce uncertainty with little potential for information gain, however, they increase the stability of the time series.

5. Data format description

5.1 File names and vocabulary

According to Data Standards Requirements for CCI Data Producers (DSRDPv2.1) following filename convention is applied. Example filename:

<Indicative Date>[<Indicative Time>]-ESACCI-<Processing Level>_<CCI Project>-<Data Type>-<Product String>[-<Additional Segregator>][-v<GDS version>]-fv<File version>.nc

Table 5-1 *Components of Cloud_cci file names and possible assignments.*

Field name field	Description
<Indicative Date>	The identifying date for this data set. Format is YYYY[MM[DD]], where YYYY is the four digit year, MM is the two digit month from 01 to 12 and DD is the two digit day of the month from 01 to 31. The date used should best represent the observation date for the data set. It can be a year, a year and a month or a year and a month and a day.
<Indicative Time>	The identifying time for this data set in UTC. Format is [HH[MM[SS]]] where HH is the two digit hour from 00 to 23, MM is the two digit minute from 00 to 59 and SS is the two digit second from 00 to 59.
<Processing Level>	Possible assignments: **L2, L3U, L3C**
<CCI Project>	**CLOUD**
<Data Type>	**CLD_PRODUCTS** (standard, all cloud properties are included in this file. For file with only one or a subset of the cloud properties, the Data Type is e.g. COT, CTP, CFC etc.)
<Product String>	The Product String gives information about the sensor(s) and platform(s) used. It therefore depends on the processing levels: L2P, L3U and L3C: Product string is **SENSOR_PLATFORM** Examples: **AVHRR_NOAA18, MODIS_AQUA, AATSR_ENVISAT** L3S: Product string is **SENSOR_MERGED** Examples: **AVHRR_MERGED, MODIS_MERGED**
v<GDS version>	not used in Cloud_cci
fv<File Version>	File version number in the form n{1,}[.n{1,}] (That is 1 or more digits followed by optional . and another 1 or more digits.)

5.2 Data format

Cloud_cci products are provided as NetCDF (Network Common Data Format) files (http://www.unidata.ucar.edu/software/netcdf/). The data files are created following NetCDF Climate and Forecast (CF) Metadata Convention version 1.6 (http://cf-pcmdi.llnl.gov/) and NetCDF Attribute Convention for Dataset Discovery (ACDD) version 1.3.

A common NetCDF file consists of dimensions, variables, and attributes. These components can be used together to capture the meaning of data and relations among data. All Cloud_cci products files are built following the same design principles. All files contain general variables, which are common for all files, and product specific variables. Dimension of all two-dimensional fields are named *lon*, *lat*. For the Histograms, additional three dimensions for COT and CTP and Phase bins are included. General variables of each file are *time, latitude*, and *longitude* (see below).

Each variable and data fields have associated attributes which are listed in Table 5-2. Global attributes contain in each of the data files are given in

Table 5-3.

Table 5-2 *Attributes assigned to variables in NetCDF.*

Name	Description
long_name	long descriptive name
standard_name	standard name that references a description of a variable's content in the CF standard name table
units	physical unit [udunits standards]
valid_min	smallest valid value of a variable
valid_max	largest valid value of a variable
scale_factor	The data are to be multiplied by this factor after it is read.
add_offset	This number is to be added to the data after it is read. If scale_factor is present, the data are first scaled before the offset is added.
_FillValue	This number represents missing or undefined data. Missing values are to be filtered before scaling.
missing	same as _FillValue

<u>**General variables**</u>

Name	Description
time	start of averaging/composite time period [Julian Date, days elapsed since 1970-01-01 00:00:00]
lat	geographical latitude of grid-box centre [degree_north]
lon	geographical longitude of grid-box centre [degree_east]

Note, the L2 files contain two-dimensional latitude and longitude fields.

Table 5-3 *Overview of global attributes of NetCDF files of Cloud_cci cloud products and possible corresponding values.*

Name	Description
title	Title of the product. (e.g. **ESA Cloud_cci L2 product**)
institution	Institution on which the data and file was processed. E.g. **Deutscher Wetterdienst (DWD), Rutherford Appleton Laboratory (RAL)**
source	Satellite sensor(s) of which the measurements were used to create the presented data. E.g. **SLSTR, SEVIRI**
history	Date and time the file was generated and optional information on product generation. E.g. **2011-02-14 12:22:43 - Product generated from CC4CL single view v2.0**
references	Web link to reference information (e.g. http://www.esa-cloud-cci.org/)
tracking_id	Universally Unique Identifier (UUID) generated using OSSP (http://www.ossp.org/pkg/lib/uuid/)(format example: **0c9e9570---cd44---102f---8001---0050c28e1010**)
conventions	NetCDF Climate and Forecast (CF) Metadata Convention 1.6
product_version	Version of product. E.g. **1.0**
summary	Summary of the products contained. E.g. **This dataset contains Level-3 (monthly) global cloud property products from satellite observations. Level 3 data are raw observations processed to geophysical quantities, and averaged onto a regular grid.**
keywords	Specific Cloud_cci keywords. E.g. **satellite, observations, cloud properties.**
id	filename.nc
naming authority	optional
keywords_vocabolary	optional
cdm_data_type	optional
comment	“These data were produced at ESACCI as part of the ESA CLOUD_CCI project.”
date_created	Data and time the file was created. E.g. **yyyymmddThhmmssZ**
creator_name	Name of the creator (members of the Cloud_cci consortium) of the file/product. E.g. **Deutscher Wetterdienst (DWD), Rutherford Appleton Laboratory (RAL)**
creator_url	Url of creator. E.g. http://www.esa-cloud-cci.org
creator_email	contact.cloudcci@dwd.de

Name	Description
project	Climate Change Initiative --- European Space Agency
geospatial_lat_min	Minimum latitude of data fields
geospatial_lat_max	Maximum latitude of data fields
geospatial_lon_min	Minimum longitude of data fields
geospatial_lon_max	Maximum longitude of data fields
geospatial_lat_units	Unit of latitude data. E.g. **degrees_north**
geospatial_lon_units	Unit of longitude data. E.g. **degrees_east**
geospatial_vertical_min	N/A
geospatial_vertical_max	N/A
spatial_resolution	Spatial resolution of products (See Section 1.3, **Table 1-2** of PUG for more details)
time_coverage_start	Start time of temporal coverage of data. E.g.: **yyyymmddThhmmssZ**
time_coverage_end	End time of temporal coverage of data. E.g.: **yyyymmddThhmmssZ**
time_coverage_duration	Total temporal coverage of data. E.g. **P1M** for monthly files
time_coverage_resolution	Temporal resolution of data. E.g. **P1D** for daily files
standard_name_vocabulary	e.g. NetCDF Climate and Forecast (CF) Metadata Convention version 1.6
license	ESA CCI Data Policy: free and open access
platform	Platform(s) of sensors used. E.g. **Envisat, NOAA-18, AQUA, TERRA**
sensor	Sensors used to generate contained data. E.g. **AATSR, AVHRR**

6. References

ATBD-FAME-Cv5, Algorithm Theoretical Baseline Document (ATBD) FAME-C – ESA Cloud_cci, Issue 5, Revision: 0, planned date of Issue: 12/09/2017, Available at: https://climate.esa.int/en/projects/cloud/

ATBD-CC4CLv9.0, Algorithm Theoretical Baseline Document (ATBD) CC4CL – ESA Cloud_cci, Issue 9, Revision: 0, available at https://climate.esa.int/en/projects/cloud/

ATBD-CC4CL_TOA_FLUXv1.1, Algorithm Theoretical Basis Document (ATBD) of the Community Code for CLimate (CC4CL) Broadband Radiative Flux Retrieval (CC4CL-TOAFLUX) – ESA Cloud_cci, Issue 1, Revision: 0, planned date of Issue: 01/03/2016, Available at: https://climate.esa.int/en/projects/cloud/

Bodas-Salcedo, A., Webb, M.J., Bony, S., Chepfer, H., Dufresne, J.L., Klein, S.A., Zhang, Y., Marchand, R., Haynes, J.M., Pincus, R. and John, V.O., **2011**. COSP: Satellite simulation software for model assessment. Bulletin of the American Meteorological Society, 92(8), p.1023.

Bouvet M. , Adriaensen S., Barker K., Bourg L., Fougnie B., Govaerts Y., Henry P., Kent C., Smith D. and Sterckx S., "CEOS IVOS Working Group 4: Intercomparison of vicarious calibration methodologies and radiometric comparison methodologies over pseudo-invariant calibration sites", Report to CEOS IVOS, **2012**.

Carbajal Henken, C.K., Lindstrot, R., Preusker, R. and Fischer, J.: FAME-C: cloud property retrieval using synergistic AATSR and MERIS observations. Atmos. Meas. Tech., 7, 3873–3890, doi:10.5194/amt-7-3873-2014, **2014**

CECRv4, Comprehensive Error Characterization Report (CECR) – ESA Cloud_cci, Issue 4, Revision: 1, Date of Issue: 06/05/2018, Available at: https://climate.esa.int/en/projects/cloud/

Donlon, C., B. Berruti, A. Buongiorno, M.-H. Ferreira, P. Femenias, J. Frerick, P. Goryl, U. Klein, H. Laur, C. Mavrocordator, J. Nieke, H. Rebhan, B. Seitz, J. Stroede, R. Sciarra, **2012**: The Global Monitoring for Environment and Security (GMES) Sentinel-3 mission. Remote Sens. of Environ., 120, 37-57

Doelling, D., Haney, C., Bhatt, R., Scarino, B., Gopalan, A. (**2018**). Geostationary visible imager calibration for the CERES SYN1deg edition 4 product. Remote Sensing, 10(2), 288.

Eliasson, S., Karlsson, K. G., van Meijgaard, E., Meirink, J. F., Stengel, M., and Willén, U.: The Cloud_cci simulator for the ESA Cloud_cci climate data record and its application to a global and a regional climate model, Geosci. Model Dev. Discuss., https://doi.org/10.5194/gmd-2018-212, in review, **2019**.

EUMETSAT, 2010: MSG Level 1.5 Image Data Format Description, EUM/MSG/ICD/105 v6.

Fell, F., and J. **Fischer**, **2001**: Numerical simulation of the light field in the atmosphere-ocean system using the matrix-operator method. J. Quant. Spectrosc. Radiat. Transfer, 3, 351–388.

Fu, Q. and **Liou**, K. N. (1992). On the correlated k-distribution method for radiative transfer in nonhomogeneous atmospheres. J. Atmos. Sci., 49:2153–2170.

Feofilov, A. G., C. J. Stubenrauch, S. Protopapadaki, and R. Armante, **2017**: Diurnal variation of high-level clouds from a synergy of the space-borne infrared sounders AIRS and IASI: detection and radiative effects. In preparation for submission to ACPD.

Fischer, J., and H. **Grassl**, **1984**: Radiative transfer in an atmosphere-ocean system: An azimuthally dependent matrix-operator approach. Appl. Opt., 23, 1035–1039.

Gomez-Chova, L., Camps-Valls, G., Calpe, J., Munoz, J., and J. Moreno: MERIS/AATSR Synergy Algorithms for cloud screening, aerosol retrieval and atmospheric correction: Cloud Screening ATBD. University of Valencia, SYN-UV-ATBD 1.0, January **2009**

Heidinger, A.K., W.C. Straka, C.C. Molling, J.T. Sullivan and X.Q. Wu, **2010**: Deriving an inter-sensor consistent calibration for the AVHRR solar reflectance data record. Int. J. Rem. Sens.,31(24), 6493-6517.

Heymsfield, A.J., Matrosov, S. and Baum, B., **2003**. Ice water path-optical depth relationships for cirrus and deep stratiform ice cloud layers. Journal of Applied Meteorology, 42(10), pp.1369-1390.

Hollmann, R., Merchant, C.J., Saunders, R., Downy, C., Buchwitz, M., Cazenave, A., Chuvieco, E., Defourny, P., de Leeuw, G., Forsberg, R. and Holzer-Popp, T., **2013**. The ESA climate change initiative: Satellite data records for essential climate variables. Bulletin of the American Meteorological Society, 94(10), pp.1541-1552.

Hollstein, A., Fischer, J., Carbajal 5 Henken, C., and Preusker, R.: Bayesian cloud detection for MERIS, AATSR, and their combination, Atmospheric Measurement Techniques, 8, 1757–1771, doi:10.5194/amt-8-1757-2015, http://www.atmos-meas-tech.net/8/1757/2015/, **2015**.

Karlsson, K.-G.; **Johansson**, E. Multi-Sensor Calibration Studies of AVHRR-Heritage Channel Radiances Using the Simultaneous Nadir Observation Approach. Remote Sens. **2014**, 6, 1845-1862.

Lindstrot, R., Preusker, R. and Fischer, J., **2010**: The empirical correction of stray light in the MERIS oxygen A band channel, *J. Atmos. Oceanic Technol.,* 27 (7), 1185-1194.

McGarragh, G. R., Poulsen, C. A., Thomas, G. E., Povey, A. C., Sus, O., Stapelberg, S., Schlundt, C., Proud, S., Christensen, M. W., Stengel, M., Hollmann, R., and Grainger, R. G.: The Community Cloud retrieval for CLimate (CC4CL) – Part 2: The optimal estimation approach, Atmos. Meas. Tech., 11, 3397-3431, https://doi.org/10.5194/amt-11-3397-2018, **2018**.

Mittaz, P.D. and R. **Harris**, **2009**: A Physical Method for the Calibration of the AVHRR/3 Thermal IR Channels 1: The Prelaunch Calibration Data. J. Atmos. Ocean. Tech., 26, 996-1019, doi: 10.1175/2008JTECHO636.1

Pavolonis, M. J. and Heidinger, A. K.: Daytime cloud overlap detection from AVHRR and VIIRS, Journal of Applied Meteorology, 43, 762–778, **2004**.

Pavolonis, M. J., Heidinger A. K., and Uttal, T., Daytime Global Cloud Typing from AVHRR and VIIRS: Algorithm Description, Validation, and Comparisons, J. Appl. Meteor., 44, 804-826, doi:10.1175/JAM2236.1, **2005**.

Poulsen, C.A., Siddans, R., Thomas, G.E., Sayer, A.M., Grainger, R.G., Campmany, E., Dean, S.M., Arnold, C. and Watts, P.D., **2012**. Cloud retrievals from satellite data using optimal estimation: evaluation and application to ATSR. *Atmospheric Measurement Techniques*, *5*(8), pp.1889-1910.

Preusker, R., and R. **Lindstrot**, **2009**: Remote sensing of cloud-top pressure using moderately resolved measurements within the oxygen A band—A sensitivity study. J. Appl. Meteor. Climatol., 48, 1562–1574.

PUGv3.1, Product User Guide (PUG) – ESA Cloud_cci, Issue 3, Revision: 1, Date of Issue: 18/04/2017, Available at: https://climate.esa.int/en/projects/cloud/

PVIRv4.1, Product Validation and Intercomparison Report (PVIR) – ESA Cloud_cci, Issue 4, Revision: 1, Date of Issue: 18/04/2017, Available at: https://climate.esa.int/en/projects/cloud/

RAFCDRv1.0, Technical Report on AVHRR GAC FCDR generation – ESA Cloud_cci, Issue 1, Revision: 0, planned date of Issue: 06/2017. Available at: https://climate.esa.int/en/projects/cloud/

RODCv1.0, Report on Orbital Drift Correction for AVHRR – ESA Cloud_cci, Issue 1, Revision: 0, planned date of Issue: 06/2017. Available at: https://climate.esa.int/en/projects/cloud/

Rodgers, C.D. , **2000**: Inverse methods for atmospheric sounding, World Scientific Publishing Pte Ltd, New York, USA.

Smith, D. L., Delderfield, J., Drummond, D., Edwards, T., Mutlow, C. T., Read,P. D., and Toplis, G. M.: Calibration of the AATSR Instrument, Adv. Space Res., 28(1), 31--39, **2001**.

Smith, D., Poulsen, C., and Latter, B.: Calibration status of the AATSR reflectance channels, 2008 ESA MERIS/(A)ATSR Workshop, **2008**.

Stamnes K., Tsay S.C., Wiscombe W. and Jayaweera K., **1998**: Numerically stable algorithm for discrete ordinate method radiative transfer in multiple scattering and emitting layered media, Appl. Opt., 27, 2502-2509.

Stengel, M., Stapelberg, S., Sus, O., Schlundt, C., Poulsen, C., Thomas, G., Christensen, M., Carbajal Henken, C., Preusker, R., Fischer, J., Devasthale, A., Willén, U., Karlsson, K.-G., McGarragh, G. R., Proud, S., Povey, A. C., Grainger, D. G., Meirink, J. F., Feofilov, A., Bennartz, R., Bojanowski, J., and Hollmann, R.: Cloud property datasets retrieved from AVHRR, MODIS, AATSR and MERIS in the framework of the Cloud_cci project, Earth Syst. Sci. Data Discuss., https://doi.org/10.5194/essd-2017-48, in review, **2017**.

Stengel, M., Schlundt, C., Stapelberg, S., Sus, O., Eliasson, S., Willén, U., and Meirink, J. F.: Comparing ERA-Interim clouds with satellite observations using a simplified satellite simulator, Atmos. Chem. Phys., 18, 17601–17614, https://doi.org/10.5194/acp-18-17601-2018, 2018.

Stengel, M., Stapelberg, S., Sus, O., Finkensieper, S., Würzler, B., Philipp, D., Hollmann, R., Poulsen, C., Christensen, M., and McGarragh, G.: Cloud_cci Advanced Very High Resolution Radiometer post meridiem (AVHRR-PM) dataset version 3: 35-year climatology of global cloud and radiation properties, Earth Syst. Sci. Data, 12, 41–60, https://doi.org/10.5194/essd-12-41-2020, 2020.

Stephens, G. L., Gabriel, P. M., and Partain, P. T. (2001). Parameterization of Atmospheric Radiative Transfer. Part I: Validity of Simple Models. Journal of the Atmospheric Sciences, 58(22):3391–3409.

Stubenrauch, C. J., A. G. Feofilov, S. E. Protopapadaki, R. Armante, **2017**: Cloud climatologies from the InfraRed Sounders AIRS and IASI: Strengths, Weaknesses and Applications In preparation for submission to ACPD

Sus, O., Stengel, M., Stapelberg, S., McGarragh, G., Poulsen, C., Povey, A. C., Schlundt, C., Thomas, G., Christensen, M., Proud, S., Jerg, M., Grainger, R., and Hollmann, R.: The Community Cloud retrieval for CLimate (CC4CL) – Part 1: A framework applied to multiple satellite imaging sensors, Atmos. Meas. Tech., 11, 3373-3396, https://doi.org/10.5194/amt-11-3373-2018, **2018.**

Walther, A. and Heidinger, A.K., **2012**. Implementation of the daytime cloud optical and microphysical properties algorithm (DCOMP) in PATMOS-x. *Journal of Applied Meteorology and Climatology*, *51*(7), pp.1371-1390.

Watts P.D., Mutlow C.T., Baran A.J. and Zavody A.M., **1998**: Study on cloud properties derived from Meteosat Second Generation Observations. Eumetsat Report, http://www.eumetsat.de/en/area2/publications/rep_cloud.pdf.

7. Glossary

AMSR-E	Advanced Microwave Scanning Radiometer-EOS
AATSR	Advanced Along Track Scanning Radiometer
AM	Ante Meridiem
AVHRR	Advanced Very High Resolution Radiometer
BRDF	Bidirectional Reflectance Distribution Function
BT	Brightness Temperature
Calipso	Cloud-Aerosol Lidar and Infrared Pathfinder Satellite Observation
CFC	Cloud Fractional Coverage
CLOUDSAT	Cloud-Aerosol Lidar and Infrared Pathfinder Satellite Observations
CM SAF	EUMETSAT Satellite Application Facility on Climate Monitoring
CMUG	Climate Modelling User Group
CPH	Cloud Phase
COT	Cloud Optical Thickness
CTH	Cloud Top Height
CTP	Cloud Top Pressure
CTT	Cloud Top Temperature
DISORT	Discrete Ordinates Radiative Transfer
ECMWF	European Centre for Medium-Range Weather Forecasts
ECV	Essential Climate Variable
ENVISAT	Environmental Satellite
EOS	Earth Observing System
ESA	European Space Agency
FAME-C	FUB AATSR MERIS Cloud retrieval algorithm
FCDR	Fundamental Climate Data Record
GAC	Global Area Coverage – globally available AVHRR dataset with reduced resolution (4 km).
GSICS	Global Space-based Inter-Calibration System
GCOS	Global Climate Observing System
GEWEX	Global Energy and Water Cycle Experiment
JCH	Joint Cloud property Histogram
ISCCP	International Satellite Cloud Climatology Project
IWP	Ice Water Path
K	Kelvin

KNMI	Koninklijk Nederlands Meteorologisch Instituut
LUT	Look-up Table
LWP	Liquid Water Path
MERIS	Medium Resolution Imaging Spectrometer
MetOp	Meteorological Operational Satellite
MODIS	Moderate Resolution Imaging Spectroradiometer
MOMO	Matrix Operator Model
NASA	National Aeronautics and Space Administration
NCDC	National Climatic Data Center
NSIDC	National Snow and Ice Data Center
NOAA	National Oceanic & Atmospheric Administration
OLCI	Ocean Land Colour Instrument
ORAC	Oxford RAL Aerosol and Cloud Algorithm
PATMOS-x	AVHRR Pathfinder Atmospheres - Extended
PM	Post Meridiem
CER	Effective Radius
RTTOV	Radiative Transfer for (A)TOVS
SEVIRI	Spinning Enhanced Visible and Infrared Imager
SNO	Simultaneous Nadir Overpass
SMHI	Swedish Meteorological and Hydrological Institute
SLSTR	Sea and Land Surface Temperature Radiometer
TCDR	Thematic Climate Data Record
TOA	Top Of Atmosphere

Annex A – Complete description of data fields

A.1 Level 2 and Level 3U data

Level 2 variable *Dimensions: along_track, across_track*	**Level 3U variable**	**Description**
Auxiliary data fields		
satellite_zenith_view_no1	*satzen_asc/desc(time, lat, lon)*	Satellite zenith angle [deg]
solar_zenith_view_no1	*solzen_asc/desc(time, lat, lon)*	Solar zenith angle [deg]
rel_azimuth_view_no1	*relazi_asc/desc(time, lat, lon)*	Relative azimuth angle [deg]
illum	*illum_asc/desc(time, lat, lon)*	Illumination flag (1: day, 2: twilight, 3: night)
lsflag(time, lat, lon)	-	Land/sea mask (0: sea , 1: land)
lusflag	-	Land use flag
dem	-	Digital elevation model
nicemask	-	Snow/ice mask
Optimal Estimation related data fields		
costja	-	field containing the a priori cost
costjm	-	field containing the measurement cost
convergence	-	field containing the retrieval convergence flag with value 0 : converged , 1 : no convergence
niter	-	field containing the number of the retrieval iterations
qcflag	*qcflag_asc/desc(time, lat, lon)*	field containing a quality-check bit mask. With Bit 0 unused, Bits 1-5 set to 1 if state variable error out of bounds, Bit 6 set to 1 if no convergence achieved, Bit 7 set to 1 if cost too large. Bit 1=COT Bit 2=REF Bit 3=CTP Bit 4=CCT Bit 5=STEMP

Level 2 variable *Dimensions: along_track, across_track*	Level 3U variable	Description
Cloud mask		
cc_total	*cmask_asc/desc(time, lat, lon)*	Cloud mask (0: cloud free, 1: cloudy)
cc_total	*cmask_asc/desc_unc(time, lat, lon)*	Cloud mask uncertainty
cccot_pre	*cccot_asc/desc(time, lat, lon) ;*	Native output of cloud detection (represents a pseudo CALIPSO COT)
Cloud phase & type		
phase	*cph_asc/desc(time, lat, lon)*	Cloud top thermodynamic phase (1: water cloud, 2: ice cloud)
phase_pavolonis	*cty_asc/desc(time, lat, lon)*	Cloud type (0: clear,1: switched to liquid, 2: fog, 3: liquid, 4: supercooled, 5: switched to ice, 6: opaque ice, 7: cirrus, 8: overlapping, 9: probably opaque ice)
Cloud top pressure/height/temperature		
ctt	*ctt_asc/desc(time, lat, lon) ;*	Cloud top temperature [K]
ctt_uncertainty	*ctt_asc/desc_unc(time, lat, lon) ;*	Cloud top temperature uncertainty [K]
ctt_corrected	*ctt_corrected_asc/desc(time, lat, lon) ;*	Cloud top temperature corrected [K]
ctt_corrected_uncertainty	*ctt_corrected_asc/desc_unc(time, lat, lon) ;*	Cloud top temperature corrected uncertainty [K]
cth	*cth_asc/desc(time, lat, lon) ;*	Cloud top height [km]
cth_uncertainty	*cth_asc/desc_unc(time, lat, lon) ;*	Cloud top height uncertainty [km]
cth_corrected	*cth_corrected_asc/desc(time, lat, lon) ;*	Cloud top height corrected [K km
cth_corrected_uncertainty	*cth_corrected_asc/desc_unc(time, lat, lon) ;*	Cloud top height corrected uncertainty [km]
ctp	*ctp_asc/desc(time, lat, lon) ;*	Cloud top pressure [hPa]

Level 2 variable *Dimensions: along_track, across_track*	Level 3U variable	Description
ctp_uncertainty	*ctp_asc/desc_unc(time, lat, lon) ;*	Cloud top pressure uncertainty [hPa]
ctp_corrected	*ctp_corrected_asc/desc(time, lat, lon) ;*	Cloud top pressure corrected [hPa]
ctp_corrected_uncertainty	*ctp_corrected_asc/desc_unc(time, lat, lon) ;*	Cloud top pressure corrected uncertainty [hPa]
Cloud optical thickness		
cot	*cot_asc/desc(time, lat, lon)*	Cloud optical thickness
cot_uncertainty	*cot_asc/desc_unc(time, lat, lon)*	Cloud optical thickness uncertainty
Effective Radius		
cer	*cer_asc/desc(time, lat, lon)*	Cloud effective radius [µm]
cer_uncertainty	*cer_asc/desc_unc(time, lat, lon)*	Cloud effective radius uncertainty [µm]
Cloud water path		
cwp	*cwp_asc/desc(time, lat, lon)*	Cloud water path [g/m2]
cwp_uncertainty	*cwp_asc/desc_unc(time, lat, lon)*	Cloud water path uncertainty [g/m2]
Spectral cloud albedo		
cloud_albedo_in_channel_no_1	*cla_vis006_asc/desc(time, lat, lon)*	Cloud albedo at 0.6µm
cloud_albedo_uncertainty_in_ channel_no_1	*cla_vis006_asc/desc_unc(time, lat, lon)*	Cloud albedo at 0.6µm uncertainty
cloud_albedo_in_channel_no_2	*cla_vis008_asc/desc(time, lat, lon)*	Cloud albedo at 0.8µm
cloud_albedo_uncertainty_in_ channel_no_2	*cla_vis008_asc/desc_unc(time, lat, lon)*	Cloud albedo at 0.8µm uncertainty
cloud_albedo_in_channel_no_3	-	
cloud_albedo_uncertainty_in _channel_no_3	-	

Level 2 variable *Dimensions: along_track, across_track*	Level 3U variable	Description
cloud_albedo_in_channel_no_3	-	
cloud_albedo_uncertainty_in_channel_no_4	-	
Cloud effective emissivity		
cee_in_channel_no_4	-	Cloud effective emissivity at 3.7 µm
cee_uncertainty_in_channel_no_4	-	Cloud effective emissivity at 3.7 µm
cee_in_channel_no_5	*cee_asc/desc(time, lat, lon)*	Cloud effective emissivity at 10.8 µm
cee_uncertainty_in_channel_no_5	*cee_asc/desc_unc(time, lat, lon)*	Cloud effective emissivity at 10.8 µm
cee_in_channel_no_6	-	Cloud effective emissivity at 12.0 µm
cee_uncertainty_in_channel_no_6	-	Cloud effective emissivity at 12.0 µm
Surface Temperature		
stemp	stemp*_asc/desc(time, lat, lon)*	field containing the surface temperature in Kelvin
stemp_uncertainty	stemp*_asc/desc_unc(time, lat, lon)*	field containing the uncertainty of *stemp* in Kelvin
TOA broadband radiative fluxes		
toa_lwup	*toa_lwup_asc/desc(time, lat, lon)*	top of atmosphere upwelling longwave radiation, all-sky
toa_lwup_clr	*toa_lwup_clr_asc/desc (time, lat, lon)*	top of atmosphere upwelling longwave radiation, clear-sky
toa_swup	*toa_swup_asc/desc (time, lat, lon)*	top of atmosphere upwelling shortwave radiation, all-sky
toa_swup_clr	*toa_swup_clr_asc/desc (time, lat, lon)*	top of atmosphere upwelling shortwave radiation, clear-sky

Level 2 variable *Dimensions: along_track, across_track*	Level 3U variable	Description
toa_swdn	*toa_swdn_asc/desc (time, lat, lon)*	top of atmosphere downwelling shortwave radiation
BOA broadband radiative fluxes		
boa_lwdn	*boa_lwdn_asc/desc(time, lat, lon)*	bottom of atmosphere downwelling longwave radiation, all-sky
boa_lwdn_clr	*boa_lwdn_clr_asc/desc (time, lat, lon)*	bottom of atmosphere downwelling longwave radiation, clear-sky
boa_swdn	*boa_swdn_asc/desc (time, lat, lon)*	bottom of atmosphere downwelling shortwave radiation, all-sky
boa_swdn_clr	*boa_swdn_clr_asc/desc (time, lat, lon)*	bottom of atmosphere downwelling shortwave radiation, clear-sky
boa_lwup	*boa_lwup_asc/desc (time, lat, lon)*	bottom of atmosphere upwelling longwave radiation, all-sky
boa_lwup_clr	*boa_lwup_clr_asc/desc (time, lat, lon)*	bottom of atmosphere upwelling longwave radiation, clear-sky
boa_swup	*boa_swup_asc/desc (time, lat, lon)*	bottom of atmosphere upwelling shortwave radiation, all-sky
boa_swup_clr	*boa_swup_clr_asc/desc (time, lat, lon)*	bottom of atmosphere upwelling shortwave radiation, clear-sky
boa_par_dif	*boa_par_dif_asc/desc (time, lat, lon)*	bottom of atmosphere diffuse downwelling photosynthetic radiative flux
boa_par_tot	*boa_par_tot_asc/desc (time, lat, lon)*	bottom of atmosphere total downwelling photosynthetic radiative flux

A.2 Level 3C

Level-3C variable	Description
Numbers/counters used for averaging	
nobs(time, lat, lon)	Total number of observations
nobs_day(time, lat, lon)	Total number of daytime observations
nobs_clear_day(time, lat, lon)	Number of clear-sky, daytime observations
nobs_cloudy_day(time, lat, lon)	Number of cloudy, daytime observations
nobs_clear_night(time, lat, lon)	Number of clear-sky, nighttime observations
nobs_cloudy_night(time, lat, lon)	Number of cloudy, nighttime observations
nobs_clear_twl(time, lat, lon)	Number of clear-sky, twilight observations
nobs_cloudy_twl(time, lat, lon)	Number of cloudy, twilight observations
nobs_cloudy(time, lat, lon)	Total number of cloudy observations
nretr_cloudy(time, lat, lon)	Number of cloud property retrievals
nretr_cloudy_liq(time, lat, lon)	Number of cloud property retrievals for liquid clouds
nretr_cloudy_ice(time, lat, lon)	Number of cloud property retrievals for ice clouds
nretr_cloudy_day(time, lat, lon)	Number of daytime cloud property retrievals
nretr_cloudy_day_liq(time, lat, lon)	Number of daytime cloud property retrievals for liquid clouds
nretr_cloudy_day_ice(time, lat, lon)	Number of daytime cloud property retrievals for ice clouds
nretr_cloudy_low(time, lat, lon)	Number of cloud property retrievals for low clouds
nretr_cloudy_mid(time, lat, lon)	Number of cloud property retrievals for mid-level clouds
nretr_cloudy_high(time, lat, lon)	Number of cloud property retrievals for high clouds
Cloud fraction	
cfc(time, lat, lon)	Total cloud fraction - mean of individual pixel retrievals
cfc_std(time, lat, lon)	Total cloud fraction - standard deviation of individual pixel retrievals
cfc_prop_unc(time, lat, lon)	Total cloud fraction - propagated uncertainty: total uncertainty from individual pixel uncertainty added in quadrature

Level-3C variable	Description
cfc_corr_unc(time, lat, lon)	Total cloud fraction - correlated uncertainty assuming correlation of 0.1
cfc_unc(time, lat, lon)	Total cloud fraction - mean of individual pixel uncertainties
cfc_low(time, lat, lon)	Portion of total cloud fraction due to low clouds
cfc_mid(time, lat, lon)	Portion of total cloud fraction due to mid-level clouds
cfc_high(time, lat, lon)	Portion of total cloud fraction due to high clouds
cfc_day(time, lat, lon)	Total cloud fraction daytime - mean of individual pixel retrievals
cfc_night(time, lat, lon)	Total cloud fraction night time - mean of individual pixel retrievals
cfc_twl(time, lat, lon)	Total cloud fraction twilight - mean of individual pixel retrievals
Cloud phase	
cph(time, lat, lon)	Liquid cloud fraction - mean of individual pixel phase retrievals
cph_std(time, lat, lon)	Liquid cloud fraction–– standard deviation of individual pixel phase retrievals
cph_day(time, lat, lon)	Liquid cloud fraction daytime - mean of individual pixel phase retrievals
cph_day_std(time, lat, lon)	Liquid cloud fraction daytime - standard deviation of individual pixel phase retrievals
Cloud top pressure/height/temperature	
ctt(time, lat, lon)	Cloud top temperature - mean of individual pixel retrievals
ctt_std(time, lat, lon)	Cloud top temperature - standard deviation of individual pixel retrievals
ctt_prop_unc(time, lat, lon)	Cloud top temperature - propagated uncertainty: total uncertainty from individual pixel uncertainty added in quadrature
ctt_corr_unc(time, lat, lon)	Cloud top temperature - correlated uncertainty assuming correlation of 0.1
ctt_unc(time, lat, lon)	Cloud top temperature - mean of individual pixel uncertainties
ctt_corrected(time, lat, lon)	Corrected cloud top temperature - mean of corrected individual pixel retrievals
ctt_corrected_std(time, lat, lon)	Corrected cloud top temperature - standard deviation of corrected individual pixel retrievals

Level-3C variable	Description
ctt_corrected_prop_unc(time, lat, lon)	Corrected cloud top temperature - propagated uncertainty: total uncertainty from corrected individual pixel uncertainty added in quadrature
ctt_corrected_corr_unc(time, lat, lon)	Corrected cloud top temperature - correlated uncertainty assuming correlation of 0.1
ctt_corrected_unc(time, lat, lon)	Corrected cloud top temperature - mean of corrected individual pixel uncertainties
cth(time, lat, lon)	Cloud top height - mean of individual pixel retrievals
cth_std(time, lat, lon)	Cloud top height - standard deviation of individual pixel retrievals
cth_prop_unc(time, lat, lon)	Cloud top height - propagated uncertainty: total uncertainty from individual pixel uncertainty added in quadrature
cth_corr_unc(time, lat, lon)	Cloud top height - correlated uncertainty assuming correlation of 0.1
cth_unc(time, lat, lon)	Cloud top height - mean of individual pixel uncertainties
cth_corrected(time, lat, lon)	Corrected cloud top height - mean of corrected individual pixel retrievals
cth_corrected_std(time, lat, lon)	Corrected cloud top height - standard deviation of corrected individual pixel retrievals
cth_corrected_prop_unc(time, lat, lon)	Corrected cloud top height - propagated uncertainty: total uncertainty from corrected individual pixel uncertainty added in quadrature
cth_corrected_corr_unc(time, lat, lon)	Corrected cloud top height - correlated uncertainty assuming correlation of 0.1
cth_corrected_unc(time, lat, lon)	Corrected cloud top height - mean of corrected individual pixel uncertainties
ctp(time, lat, lon)	Cloud top pressure - mean of individual pixel retrievals
ctp_std(time, lat, lon)	Cloud top pressure - standard deviation of individual pixel retrievals
ctp_prop_unc(time, lat, lon)	Cloud top pressure - propagated uncertainty: total uncertainty from individual pixel uncertainty added in quadrature
ctp_corr_unc(time, lat, lon)	Cloud top pressure - correlated uncertainty assuming correlation of 0.1
ctp_unc(time, lat, lon)	Cloud top pressure - mean of individual pixel uncertainties
ctp_log(time, lat, lon)	Cloud top pressure - logarithmic mean of individual pixel retrievals
ctp_corrected(time, lat, lon)	Corrected cloud top pressure - mean of corrected individual pixel retrievals

Level-3C variable	Description
ctp_corrected_std(time, lat, lon)	Corrected cloud top pressure - standard deviation of corrected individual pixel retrievals
ctp_corrected_prop_unc(time, lat, lon)	Corrected cloud top pressure - propagated uncertainty: total uncertainty from corrected individual pixel uncertainty added in quadrature
ctp_corrected_corr_unc(time, lat, lon)	Corrected cloud top pressure - correlated uncertainty assuming correlation of 0.1
ctp_corrected_unc(time, lat, lon)	Corrected cloud top pressure - mean of corrected individual pixel uncertainties
Surface temperature	
stemp(time, lat, lon)	Surface temperature - mean of individual pixel retrievals
stemp_std(time, lat, lon)	Surface temperature - standard deviation of individual pixel retrievals
stemp_prop_unc(time, lat, lon)	Surface temperature - propagated uncertainty: total uncertainty from individual pixel uncertainty added in quadrature
stemp_corr_unc(time, lat, lon)	Surface temperature - correlated uncertainty assuming correlation of 0.1
stemp_unc(time, lat, lon)	Surface temperature - mean of individual pixel uncertainties
Cloud effective radius	
cer(time, lat, lon)	Cloud effective radius - mean of individual pixel retrievals
cer_std(time, lat, lon)	Cloud effective radius - standard deviation of individual pixel retrievals
cer_prop_unc(time, lat, lon)	Cloud effective radius - propagated uncertainty: total uncertainty from individual pixel uncertainty added in quadrature
cer_corr_unc(time, lat, lon)	Cloud effective radius - correlated uncertainty assuming correlation of 0.1
cer_unc(time, lat, lon)	Cloud effective radius - mean of individual pixel uncertainties
cer_liq(time, lat, lon)	Liquid cloud effective radius - mean of individual pixel retrievals
cer_liq_std(time, lat, lon)	Liquid cloud effective radius - standard deviation of individual pixel retrievals
cer_liq_prop_unc(time, lat, lon)	Liquid cloud effective radius - propagated uncertainty: total uncertainty from individual pixel uncertainty added in quadrature
cer_liq_corr_unc(time, lat, lon)	Liquid cloud effective radius - correlated uncertainty assuming

Level-3C variable	Description
	correlation of 0.1
cer_liq_unc(time, lat, lon)	Liquid cloud effective radius - mean of individual pixel uncertainties
cer_ice(time, lat, lon)	Ice cloud effective radius - mean of individual pixel retrievals
cer_ice_std(time, lat, lon)	Ice cloud effective radius - standard deviation of individual pixel retrievals
cer_ice_prop_unc(time, lat, lon)	Ice cloud effective radius - propagated uncertainty: total uncertainty from individual pixel uncertainty added in quadrature
cer_ice_corr_unc(time, lat, lon)	Ice cloud effective radius - correlated uncertainty assuming correlation of 0.1
cer_ice_unc(time, lat, lon)	Ice cloud effective radius - mean of individual pixel uncertainties
Cloud optical thickness	
cot(time, lat, lon)	Cloud optical thickness - mean of individual pixel retrievals
cot_log(time, lat, lon)	Cloud optical thickness - logarithmic mean of individual pixel retrievals
cot_std(time, lat, lon)	Cloud optical thickness - standard deviation of individual pixel retrievals
cot_prop_unc(time, lat, lon)	Cloud optical thickness - propagated uncertainty: total uncertainty from individual pixel uncertainty added in quadrature
cot_corr_unc(time, lat, lon)	Cloud optical thickness - correlated uncertainty assuming correlation of 0.1
cot_unc(time, lat, lon)	Cloud optical thickness - mean of individual pixel uncertainties
cot_liq(time, lat, lon)	Liquid cloud optical thickness- mean of individual pixel retrievals
cot_liq_std(time, lat, lon)	Liquid cloud optical thickness - standard deviation of individual pixel retrievals
cot_liq_prop_unc(time, lat, lon)	Liquid cloud optical thickness - propagated uncertainty: total uncertainty from individual pixel uncertainty added in quadrature
cot_liq_corr_unc(time, lat, lon)	Liquid cloud optical thickness - correlated uncertainty assuming correlation of 0.1
cot_liq_unc(time, lat, lon)	Liquid cloud optical thickness - mean of individual pixel uncertainties
cot_ice(time, lat, lon)	Ice cloud optical thickness - mean of individual pixel retrievals
cot_ice_std(time, lat, lon)	Ice cloud optical thickness - standard deviation of individual pixel

Level-3C variable	Description
	retrievals
cot_ice_prop_unc(time, lat, lon)	Ice cloud optical thickness - propagated uncertainty: total uncertainty from individual pixel uncertainty added in quadrature
cot_ice_corr_unc(time, lat, lon)	Ice cloud optical thickness - correlated uncertainty assuming correlation of 0.1
cot_ice_unc(time, lat, lon)	Ice cloud optical thickness - mean of individual pixel uncertainties
Cloud effective emissivity	
cee(time, lat, lon)	Cloud effective emissivity at 10.8 µm - mean of individual pixel retrievals
cee_std(time, lat, lon)	Cloud effective emissivity at 10.8 µm - standard deviation of individual pixel retrievals
cee_prop_unc(time, lat, lon)	Cloud effective emissivity at 10.8 µm - propagated uncertainty: total uncertainty from individual pixel uncertainty added in quadrature
cee_corr_unc(time, lat, lon)	Cloud effective emissivity at 10.8 µm - correlated uncertainty assuming correlation of 0.1
cee_unc(time, lat, lon)	Cloud effective emissivity at 10.8 µm - mean of individual pixel uncertainties
Spectral cloud albedo	
cla_vis006(time, lat, lon)	Cloud albedo at 0.6 µm - mean of individual pixel retrievals
cla_vis006_std(time, lat, lon)	Cloud albedo at 0.6 µm - standard deviation of individual pixel retrievals
cla_vis006_prop_unc(time, lat, lon)	Cloud albedo at 0.6 µm - propagated uncertainty: total uncertainty from individual pixel uncertainty added in quadrature
cla_vis006_corr_unc(time, lat, lon)	Cloud albedo at 0.6 µm - correlated uncertainty assuming correlation of 0.1
cla_vis006_unc(time, lat, lon)	Cloud albedo at 0.6 µm - mean of individual pixel uncertainties
cla_vis006_liq(time, lat, lon)	Liquid cloud albedo at 0.6 µm - mean of individual pixel retrievals
cla_vis006_liq_std(time, lat, lon)	Liquid cloud albedo at 0.6 µm - standard deviation of individual pixel retrievals
cla_vis006_liq_unc(time, lat, lon)	Liquid cloud albedo at 0.6 µm - mean of individual pixel uncertainties
cla_vis006_ice(time, lat, lon)	Ice cloud albedo at 0.6 µm - mean of individual pixel retrievals

Level-3C variable	Description
cla_vis006_ice_std(time, lat, lon)	Ice cloud albedo at 0.6 µm - standard deviation of individual pixel retrievals
cla_vis006_ice_unc(time, lat, lon)	Ice cloud albedo at 0.6 µm - mean of individual pixel uncertainties
cla_vis008(time, lat, lon)	Cloud albedo at 0.8 µm - mean of individual pixel retrievals
cla_vis008_std(time, lat, lon)	Cloud albedo at 0.8 µm - standard deviation of individual pixel retrievals
cla_vis008_prop_unc(time, lat, lon)	Cloud albedo at 0.8 µm - propagated uncertainty: total uncertainty from individual pixel uncertainty added in quadrature
cla_vis008_corr_unc(time, lat, lon)	Cloud albedo at 0.8 µm - correlated uncertainty assuming correlation of 0.1
cla_vis008_unc(time, lat, lon)	Cloud albedo at 0.8 µm - mean of individual pixel uncertainties
cla_vis008_liq(time, lat, lon)	Liquid cloud albedo at 0.8 µm - mean of individual pixel retrievals
cla_vis008_liq_std(time, lat, lon)	Liquid cloud albedo at 0.8 µm - standard deviation of individual pixel retrievals
cla_vis008_liq_unc(time, lat, lon)	Liquid cloud albedo at 0.8 µm - mean of individual pixel uncertainties
cla_vis008_ice(time, lat, lon)	Ice cloud albedo at 0.8 µm - mean of individual pixel retrievals
cla_vis008_ice_std(time, lat, lon)	Ice cloud albedo at 0.8 µm - standard deviation of individual pixel retrievals
cla_vis008_ice_unc(time, lat, lon)	Ice cloud albedo at 0.8 µm - mean of individual pixel uncertainties
Cloud water path	
lwp(time, lat, lon)	Cloud liquid water path - mean of individual pixel retrievals
lwp_std(time, lat, lon)	Cloud liquid water path - standard deviation of individual pixel retrievals
lwp_prop_unc(time, lat, lon)	Cloud liquid water path - propagated uncertainty: total uncertainty from individual pixel uncertainty added in quadrature
lwp_corr_unc(time, lat, lon)	Cloud liquid water path - correlated uncertainty assuming correlation of 0.1
lwp_unc(time, lat, lon)	Cloud liquid water path - mean of individual pixel uncertainties
lwp_allsky(time, lat, lon)	Cloud liquid water path all-sky - grid box mean of individual pixel retrievals, including clear-sky pixels
iwp(time, lat, lon)	Cloud ice water path - mean of individual pixel retrievals

Level-3C variable	Description
iwp_std(time, lat, lon)	Cloud ice water path - standard deviation of individual pixel retrievals
iwp_prop_unc(time, lat, lon)	Cloud ice water path - propagated uncertainty: total uncertainty from individual pixel uncertainty added in quadrature
iwp_corr_unc(time, lat, lon)	Cloud ice water path - correlated uncertainty assuming correlation of 0.1
iwp_unc(time, lat, lon)	Cloud ice water path - mean of individual pixel uncertainties
iwp_allsky(time, lat, lon)	Cloud ice water path all-sky - grid box mean of individual pixel retrievals, including clear-sky pixels
TOA broadband radiative fluxes	
toa_lwup(time, lat, lon)	top of atmosphere upwelling longwave radiation, all-sky
toa_lwup_clr(time, lat, lon)	top of atmosphere upwelling longwave radiation, clear-sky
toa_swup(time, lat, lon)	top of atmosphere upwelling shortwave radiation, all-sky
toa_swup_clr(time, lat, lon)	top of atmosphere upwelling shortwave radiation, clear-sky
toa_swdn(time, lat, lon)	top of atmosphere downwelling shortwave radiation
toa_lwup_low(time, lat, lon)	top of atmosphere upwelling longwave radiation, all-sky + low clouds
toa_lwup_mid(time, lat, lon)	top of atmosphere upwelling longwave radiation, all-sky + mid-level clouds
toa_lwup_hig(time, lat, lon)	top of atmosphere upwelling longwave radiation, all-sky + high clouds
toa_swup_low(time, lat, lon)	top of atmosphere upwelling shortwave radiation, all-sky + low clouds
toa_swup_mid(time, lat, lon)	top of atmosphere upwelling shortwave radiation, all-sky + mid-level clouds
toa_swup_hig(time, lat, lon)	top of atmosphere upwelling shortwave radiation, all-sky + high clouds
BOA broadband radiative fluxes	
boa_lwdn(time, lat, lon)	bottom of atmosphere downwelling longwave radiation, all-sky
boa_lwdn_clr(time, lat, lon)	bottom of atmosphere downwelling longwave radiation, clear-sky
boa_swdn(time, lat, lon)	bottom of atmosphere downwelling shortwave radiation, all-sky
boa_swdn_clr(time, lat, lon)	bottom of atmosphere downwelling shortwave radiation, clear-sky
boa_lwup(time, lat, lon)	bottom of atmosphere upwelling longwave radiation, all-sky
boa_lwup_clr(time, lat, lon)	bottom of atmosphere upwelling longwave radiation, clear-sky
boa_swup(time, lat, lon)	bottom of atmosphere upwelling shortwave radiation, all-sky
boa_swup_clr(time, lat, lon)	bottom of atmosphere upwelling shortwave radiation, clear-sky
boa_par_dif(time, lat, lon)	bottom of atmosphere diffuse downwelling photosynthetic radiative flux

Level-3C variable	Description
boa_par_tot(time, lat, lon)	bottom of atmosphere total downwelling photosynthetic radiative flux
Histograms	
hist2d_cot_ctp(time, hist_phase, hist2d_ctp_bin_centre, hist2d_cot_bin_centre, lat, lon)	Two-dimensional, COT-CTP histogram containing absolute counts
hist2d_ctp_bin_centre	Center of CTP bins in 2-dim COT-CTP histogram
hist2d_cot_bin_centre	Center of COT bins in 2-dim COT-CTP histogram
hist2d_ctp_bin_border	Borders of CTP bins in 2-dim COT-CTP histogram
hist2d_cot_bin_border	Borders of COT bins in 2-dim COT-CTP histogram
hist1d_cot(time, hist_phase, hist1d_cot_bin_centre, lat, lon)	1-dimensional histogram of cloud optical thickness per grid cell
hist1d_cot_bin_centre	Center of COT bins in 1-dim COT histogram
hist1d_cot_bin_border	Borders of COT bins in 1-dim COT histogram
hist1d_ctp(time, hist_phase, hist1d_ctp_bin_centre, lat, lon)	1-dimensional histogram of cloud top pressure per grid cell
hist1d_ctp_bin_centre	Center of CTP bins in 1-dim CTP histogram
hist1d_ctp_bin_border	Borders of CTP bins in 1-dim CTP histogram
hist1d_ctt(time, hist_phase, hist1d_ctt_bin_centre, lat, lon)	1-dimensional histogram of cloud top temperature per grid cell
hist1d_ctt_bin_centre	Center of CTT bins in 1-dim CTT histogram
hist1d_ctt_bin_border	Borders of CTT bins in 1-dim CTT histogram
hist1d_cer(time, hist_phase, hist1d_cer_bin_centre, lat, lon)	1-dimensional histogram of cloud effective radius per grid cell
hist1d_cer_bin_centre	Center of CER bins in 1-dim CER histogram
hist1d_cer_bin_border	Borders of CER bins in 1-dim CER histogram
hist1d_cwp(time, hist_phase, hist1d_cwp_bin_centre, lat, lon)	1-dimensional histogram of cloud water path per grid cell
hist1d_cwp_bin_centre	Center of CWP bins in 1-dim CWP histogram
hist1d_cwp_bin_border	Borders of CWP bins in 1-dim CWP histogram

Level-3C variable	Description
hist1d_cla_vis006(time, hist_phase, hist1d_cla_vis006_bin_centre, lat, lon)	1-dimensional histogram of cloud albedo at 0.6µm per grid cell
hist1d_cla_vis006_bin_centre	Center of CLA_vis006 bins in 1-dim CLA_vis006 histogram
hist1d_cla_vis006_bin_border	Borders of CLA_vis006 bins in 1-dim CLA_vis006 histogram
hist1d_cla_vis008(time, hist_phase, hist1d_cla_vis008_bin_centre, lat, lon)	1-dimensional histogram of cloud albedo at 0.8µm per grid cell
hist1d_cla_vis008_bin_centre	Center of CLA_vis008 bins in 1-dim CLA_vis008 histogram
hist1d_cla_vis008_bin_border	Borders of CLA_vis008 bins in 1-dim CLA_vis008 histogram